European Journal of Inflammation

Original article

European Journal of Inflammation
2016, Vol. 14(3) 169–183

DOI: 10.1177/1721727X16677763
eji.sagepub.com
SAGE

Improved corrosion resistance and biocompatibility of a calcium phosphate coating on a magnesium alloy for orthopedic applications

Yongping Wang,[1,2] Zhaojin Zhu,[1] Xiangyang Xu,[1] Yaohua He[3] and Bingchun Zhang[4]

Abstract

In this study a calcium phosphate (Ca–P) coating was fabricated on the surface of an AZ31 alloy by a chemical deposition process, and the in vitro and in vivo studies were carried out on a Ca–P-coated and uncoated AZ31 alloy to determine the effect of Ca–P coating on the corrosion behavior and biocompatibility of the AZ31 alloy. The morphology and composition of the Ca–P coating were characterized by scanning electron microscopy and energy dispersive spectroscopy. The corrosion behavior of the Ca-P coating was evaluated by a static immersion test and the effects of the Ca–P coating on biocompatibility were also investigated by in vitro cell experiments and in vivo animal experiments. The results indicated that the Ca–P coating reduced the in vitro and in vivo corrosion rates of the AZ31 alloy. Cell experiments showed significantly good adherence and high proliferation on the Ca–P-coated AZ31 alloy than those on the uncoated AZ31 alloy ($P < 0.05$). The blood cell aggregation tests showed that the Ca–P-coated AZ31 alloy had decreased the blood cell aggregation compared to the uncoated AZ31 alloy. The animal experiments showed that the uncoated AZ31 alloy degraded more rapidly than the Ca–P-coated AZ31 alloy and the Ca–P coating provided significantly good biocompatibility, thus suggesting that the Ca–P coating not only slowed down the corrosion rate of the AZ31 alloy, but also improved its biocompatibility. Therefore, the Ca–P-coated AZ31 alloy can be considered as a promising biomaterial for orthopedic applications.

Keywords

biocompatibility, calcium phosphate coating, corrosion resistance, degradation, magnesium alloy

Date received: 19 September 2016; accepted: 12 October 2016

Introduction

In recent years, magnesium alloys have been considered as candidate degradable medical biomaterials for orthopedic application, thus attracting attention due not only to the degradability, but also to the suitable mechanical properties and good biocompatibility.[1–10] Until now, many different kinds of magnesium alloys, such as AZ31,[11] AZ91,[11] WE43,[11] WE54,[12] Mg–Y–Zn,[13] Mg–Zn,[4] Mg–Ca,[6,14] and Mg–Zn–Ca[7,15] and Mg-Nd-Zn-Zr,[16–18] have been investigated as potential implant materials. A series of studies have confirmed that magnesium alloys have good biocompatibility, may promote osteocyte growth, and induce production of osteoblasts and osteocytes.[19–21] Unfortunately, a high corrosion rate in the physiologic environment,

[1]Department of Orthopedics, Shanghai Jiao Tong University Medical School Affiliated Ruijin Hospital, Shanghai, China
[2]Department of Orthopaedics, First Hospital of Lanzhou University, Lanzhou, China
[3]Department of Orthopaedics, Sixth People's Hospital of Shanghai JiaoTong University, Shanghai, China
[4]Institute of Metal Research, Chinese Academy of Sciences, Shenyang, China

Corresponding author:
Xiangyang Xu, Shanghai Jiao Tong University Medical School Affiliated Ruijin Hospital, No.197, Rui Jin Er Road, Shanghai, 200025, China.
Email: xuxy664531@163.com

Table 1. Chemical composition of the AZ31 alloy.

Materials	Chemical composition (wt.%)							
	Mg	Al	Zn	Mn	Si	Ni	Cu	Fe
AZ31	Balance	1.92	0.74	0.35	0.026	0.0003	0.0028	<0.003

Table 2. Chemical composition of the mixed solution.

Composition	$NaNO_3$	$Ca(H_2PO_4)_2{\cdot}H_2O$	30%H_2O_2
Concentration	55.5 g/L	99.7 g/L	185.1 mL/L

resulting in the generation of generous hydrogen gas and rapid loss of mechanical strength, is the major obstacle to the clinical use of magnesium alloys.[3,5,19,20,22,23] Hence, if magnesium alloys are to be used successfully in orthopedic applications, the corrosion rates must be effectively controlled so as not to exceed the healing rates of the affected tissues. Thus, the magnesium alloys should remain present in the body and maintain mechanical integrity until the affected tissues have healed. As biomaterials for orthopedic applications, the biocompatibility and surface bioactivity of magnesium alloys must be taken into consideration. To further improve the corrosion resistance and surface biocompatibility of AZ31 alloy, a calcium phosphate (Ca–P) coating was fabricated on the surface of the AZ31 alloy by a chemical deposition process. However, the Ca–P-coated AZ31 alloy has not been systematically studied as a degradable biomaterial for orthopedic applications in vitro or in vivo. In the current study, we focused on the influence of the Ca–P coating on the corrosion behavior and biocompatibility of the AZ31 alloy. The aim of the present study was to determine the feasibility of the Ca–P coating in controlling the corrosion rate and improving the surface biocompatibility of the AZ31 alloy under in vitro and in vivo conditions.

Materials and methods

Materials

AZ31 alloy was obtained from the Institute of Metal Research (Chinese Academy of Sciences). The chemical composition of the AZ31 alloy is listed in Table 1.

Dulbecco Modified Eagle Medium (DMEM) (Hyclone, USA) without fetal bovine serum (FBS) was used as the corrosion medium.

MC_3T_3-E_1 cells were provided by the Chinese Academy of Sciences Type Culture Collection (China).

Healthy New Zealand white rabbits weighing 2.5 ± 0.3 kg were supplied by the Shanghai Jiesijie Lab. Animal Co., Ltd. (license no. SCXK [hu] 2010-0026; Shanghai, China).

Sample preparation

The disc samples for the in vitro experiments (10 mm in diameter and 2 mm in thickness) and plate samples for the in vivo study (35 mm in length, 5 mm in width, and 2 mm in thickness) were machined from the extruded AZ31 alloy ingot. The AZ31 alloy samples were mechanically polished up to 1000 grits, then ultrasonically cleaned in ethanol and dried at room temperature. All samples were sterilized with ethylene oxide prior to the experiments.

Ca–P coating treatment

Coating was carried out using a chemical deposition method. The samples were first immersed in 40% hydrofluoric acid at room temperature for 6 h. Subsequently, the samples were cleaned in deionized water. Then, the samples were immersed in a mixed solution for 24 h at 20°C for Ca–P coating treatment to obtain a Ca–P coating on the surface of the samples. Table 2 lists the chemical composition of the mixed solution.

Coating characterization

Scanning electron microscopy (SEM, Hitachi, S-4800; Japan) was used to visualize the surface morphology of the Ca–P-coated AZ31 alloy. The chemical composition of the Ca–P coating was determined by energy disperse spectrometry (EDS).

In vitro corrosion test

To evaluate the in vitro corrosion behavior of the Ca–P-coated AZ31 alloy, an immersion test was performed in DMEM. Six each of the Ca–P-coated and uncoated AZ31 alloy samples were individually immersed in DMEM at 37°C, according to ASTM-G31-72.[24] After immersion for 10, 20, or 30 days, the samples were removed from the DMEM, gently rinsed with distilled water, cleaned with ethanol, and dried in air. The samples were then cleaned with 200 g/L of boiled CrO_3 solution to remove the corrosion products. Then, the corrosion morphologies were characterized by SEM, and the corrosion rates were determined by the weight loss.

In vitro cell experiment

Cytotoxicity test. The MTT assay was used to determine the cytotoxicity of the Ca–P-coated AZ31 alloy to MC_3T_3-E_1 cells.[25] The test was carried out using an indirect method in which extracts were prepared using DMEM without FBS as the extraction medium, with a ratio of the area of the sample-to-the volume of the extraction medium equal to 1.25 cm^2/mL at 37°C for 24 h.[25,26] Extracts of 25%, 50%, or 75% concentration were then prepared by dilution with fresh DMEM. Simple DMEM was chosen as the negative control and DMEM containing 0.64% phenol was the positive control.

When the MTT test was conducted, MC_3T_3-E_1 cells were incubated in 96-well cell culture plates (Costar, USA) at 5×10^4 cells/mL in each well, and incubated for 24 h to allow attachment. Then, the cell culture medium was replaced with 100 μL of 25%, 50%, 75%, or 100% extract. After 1, 3, and 5 days of culture, 20 μL of MTT (5 g/L; Sigma, St. Louis, MO, USA) was added to each well and incubated at 37°C for 4 h, then the MTT was aspirated and 150 μL of dimethyl sulfoxide (Sigma, USA) was added to each well for 15 min. The optical density (OD) was measured with a spectrophotometer (Wellscan MK3; Labsystem, Finland) at a wavelength of 492 nm to evaluate the cell viability in comparison to the control group.

Cell adhesion. For the cell adhesion assay, acridine orange (Sigma, USA) staining was used to evaluate the cell number attached on the surface of the Ca–P-coated AZ31 alloy. Six each of the Ca–P-coated and uncoated AZ31 alloy samples were placed on the bottom of a 24-well cell culture plate, and a 1-mL cell suspension (5×10^4 cells/mL) was seeded onto each sample. After culture for 6, 12, and 24 h, the samples were thrice-washed with phosphate buffered saline to remove unattached cells. The attached cells on the surface of the Ca–P-coated and uncoated AZ31 alloy samples were fixed using 95% ethanol, then stained with 0.01% acridine orange for 10 min. Stained cells were observed using a fluorescence microscope (Olympus, IX71; Japan). Cell counts were conducted at five different locations of the surface of each sample.

Cell proliferation. Aliquots (1 mL) of a cell suspension (5×10^4 cells/mL) were seeded onto Ca–P-coated and uncoated AZ31 alloy samples in 24-well plates. The culture medium was changed every 3 days. After 1, 3, and 5 days of culture, cells were detached from the samples with 0.25% trypsin-EDTA. After brief centrifugation, cells were resuspended in 1 mL of fresh DMEM and the cell number was counted using a hemacytometer.

Blood cell aggregation. Aggregations of blood cells, including red blood corpuscles (RBCs), white blood corpuscles (WBCs), and platelets, were evaluated using a blood cell count method. Fresh arterial blood (3 mL) from a healthy New Zealand white rabbit was collected into a tube that contained 0.5 mL of potassium oxalate (20 g/L) anticoagulant. Then, six each of the Ca–P-coated and uncoated AZ31 alloy samples were individually immersed in blood immediately. Prior to and after immersion for 8 min, the number of RBCs, WBCs, and platelets were measured using an automatic hematology analyzer (Sysmex, XT-1800i; Japan).[27]

In vivo study

Animal experiments. Protocols were performed in accordance with the Guidance Suggestions for the Care and Use of Laboratory Animals, issued by the Ministry of Science and Technology of the People's Republic of China (2006-09-30), and permission was obtained from the Ethic Committees of the Sixth People's Hospital of Shanghai Jiao Tong University (Shanghai, China).

The 54 New Zealand white rabbits (mean weight, 2.5 ± 0.3 kg) were randomly divided into the following three groups: the Ca–P-coated AZ31 alloy

group; the uncoated AZ31 alloy group; and the sham-operated group. After anesthetized intramuscularly with xylazine (4 mg/kg) and ketamine (8 mg/kg), the operative site on the New Zealand white rabbit was shaved. Following fixation, iodophors were utilized to sterilize the skin. Hole sheets were paved. A longitudinal incision (approximately 4 cm) was made on the medial aspect of the left proximal tibia. Under sterile conditions, the skin and subcutaneous tissue were incised to expose the proximal tibia, and the tunnel was created using an electric drill. Then, Ca–P-coated AZ31 alloy plates were implanted into the proximal tibia in the Ca–P-coated AZ31 alloy group, the uncoated AZ31 alloy plates were implanted into the uncoated AZ31 alloy group, and a bone tunnel was established in the sham-operated group (Figure 1). After saline irrigation, the wound was sutured layer by layer, and a proper dressing was applied over the incision. All of the animals received an intramuscular injection of penicillin for 3 days as an antibiotic prophylaxis after surgery. Postoperatively, the New Zealand white rabbits were allowed to move freely in their cages with no external support. The New Zealand white rabbit diet, activity, inflammatory reactions, and exudation in the incised openings were observed. Clinical examinations of the left tibia were performed every day after the operation.

Radiologic examination. X-ray radiography was performed at the operative site at 1, 2, 4, 8, and 12 weeks postoperatively to ensure the correct position of the implant and monitor the in vivo corrosion behavior of the Ca–P-coated AZ31 alloy implant.

Blood examination. To observe systemic toxic effects after implantation of the Ca–P-coated and uncoated AZ31 alloy, blood examinations were performed prior to surgery, and 1 day, and 1, 2, 4, 8, and 12 weeks after the operation to determine the serum alanine transaminase (ALT), aspartate transaminase (AST), creatinine (CREA), blood urea nitrogen (BUN), and creatine kinase (CK) using an automatic blood biochemistry analyzer (Hitachi, 7600-020; Japan).

Histopathologic examination. Six New Zealand white rabbits from each group were sacrificed by overdose of ketamine at 4, 8, or 12 weeks postoperatively. The heart, liver, and kidneys were harvested and fixed with 4% formaldehyde solution for 24 h, then embedded in paraffin wax. Each specimen was consecutively cut into slices (5 μm thick). The slices were stained using hematoxylin and eosin (HE) and the pathologic changes in the organs were observed under an optical microscope (Olympus, BX51; Japan).

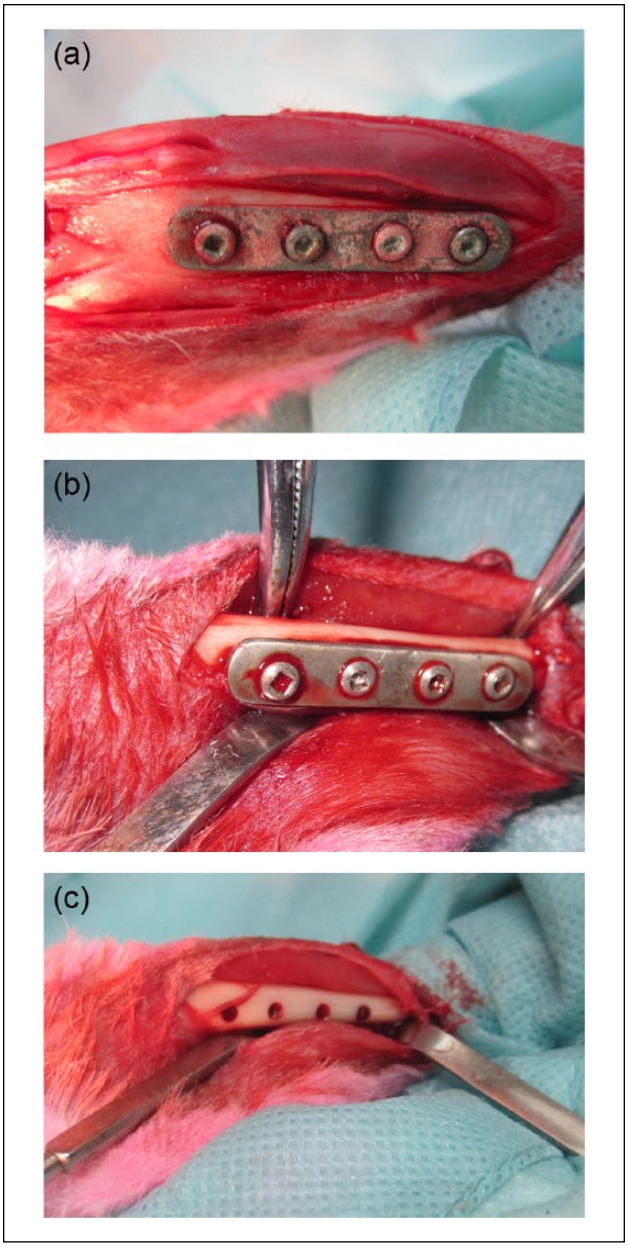

Figure 1. Surgical procedure of the animal experiments. (a) Ca–P-coated AZ31 alloy implanted into one tibia of a rabbit; (b) uncoated AZ31 alloy implanted into one tibia of a rabbit; (c) a bone tunnel was established in one tibia of a rabbit.

Statistical analysis

Statistical analysis was conducted using SPSS 13.0 (SPSS, Inc., Chicago, IL, USA). All data were

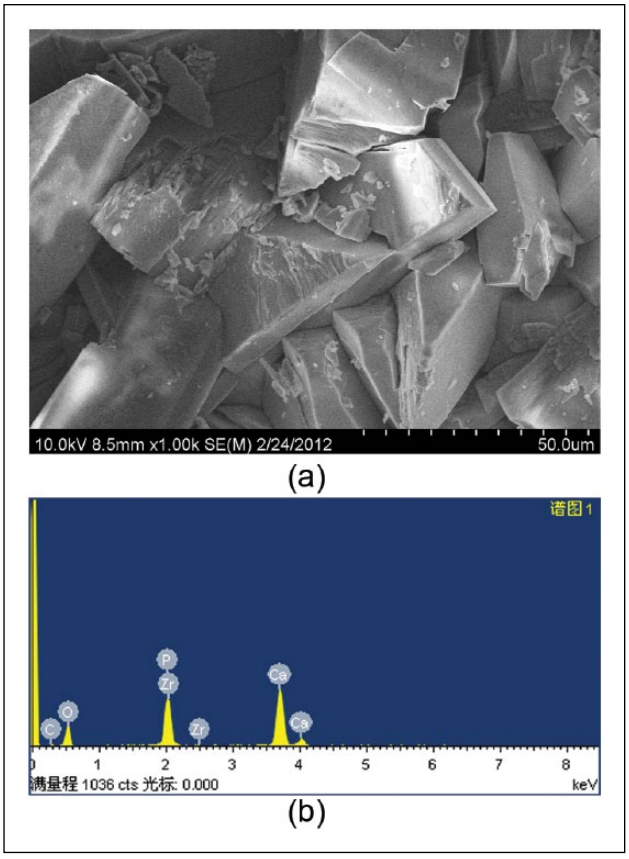

Figure 2. SEM and EDS results of the Ca–P-coated AZ31 samples. (a) SEM surface morphology of the Ca–P-coated AZ31 samples; (b) EDS spectrum of the Ca–P-coated AZ31 samples.

expressed as the mean ± SD. The differences between two groups were analyzed by an independent samples *t*-test. The differences in more than two groups were analyzed by analysis of variance (ANOVA). A P value <0.05 indicates statistically significant differences.

Results

Coating characterization

Figure 2 shows the SEM and EDS results of the Ca–P-coated AZ31 alloy. Particles shaped like flakes were clearly observed on the surface of the Ca–P-coated AZ31 alloy under SEM (Figure 2a). As shown in Figure 2b, the EDS results indicated that the particles were mainly composed of calcium, phosphate, oxygen, and carbon.

In vitro corrosion behavior

The in vitro corrosion behavior of the Ca–P-coated AZ31 alloy was evaluated by an immersion test in DMEM. Figure 3 shows the surface morphology of the Ca–P-coated and uncoated AZ31 alloy samples after a 30-day immersion in DMEM. There was a layer of corrosion products on the surface of the Ca–P-coated and uncoated AZ31 alloy (Figure 3a, b). EDS analysis revealed that the elemental composition of the corrosion products formed on the surface of the Ca–P-coated AZ31 alloy was mainly composed of oxygen, carbon, calcium, phosphate, magnesium, sodium, and chlorine (Table 3). As shown in Figure 3c and d, corrosion pits are clearly seen on the surface of the Ca–P-coated and uncoated AZ31 alloy after the corrosion products were removed; however, the corrosion pits on the surface of the Ca–P-coated AZ31 alloy were smaller and more evenly distributed than those on the surface of the uncoated AZ31 alloy, suggesting that the uncoated AZ31 alloy underwent severe pitting and general corrosion.

The corrosion rates of the Ca–P-coated and uncoated AZ31 alloy after 10, 20, or 30 days of immersion in DMEM are shown in Figure 4. The total weight lost from the uncoated AZ31 alloy was approximately 26.21% after 30 days of immersion; however, the total weight lost for the Ca–P-coated AZ31 alloy was 10.38%. The Ca–P-coated AZ31 alloy corroded much more slowly than the uncoated AZ31 alloy after 30 days of immersion in DMEM (P <0.05), indicating that the Ca–P coating significantly retarded the corrosion rate of the AZ31 alloy.

In vitro cell experiment

Cytotoxicity test. The results of the optical density (OD) and relative growth rate (RGR) based on the cytotoxicity test are listed in Table 4. As shown in Table 4, the RGR of MC_3T_3-E_1 cells in different extracts were all >75% at each time point, suggesting that the grade of cytotoxicity was 0–1 at 1, 3, and 5 days of culture in different extracts from the Ca–P-coated AZ31 alloy.

Cell adhesion. Figure 5 shows the results of acridine orange staining, displaying a significant increase in the number of cells adhering on the surface of the Ca–P-coated AZ31 alloy samples compared to the uncoated AZ31 alloy samples. The cell number adherent to the Ca–P-coated and uncoated AZ31 alloy samples were counted after 6, 12, and 24 h of culture, and the results are shown in Figure 6.

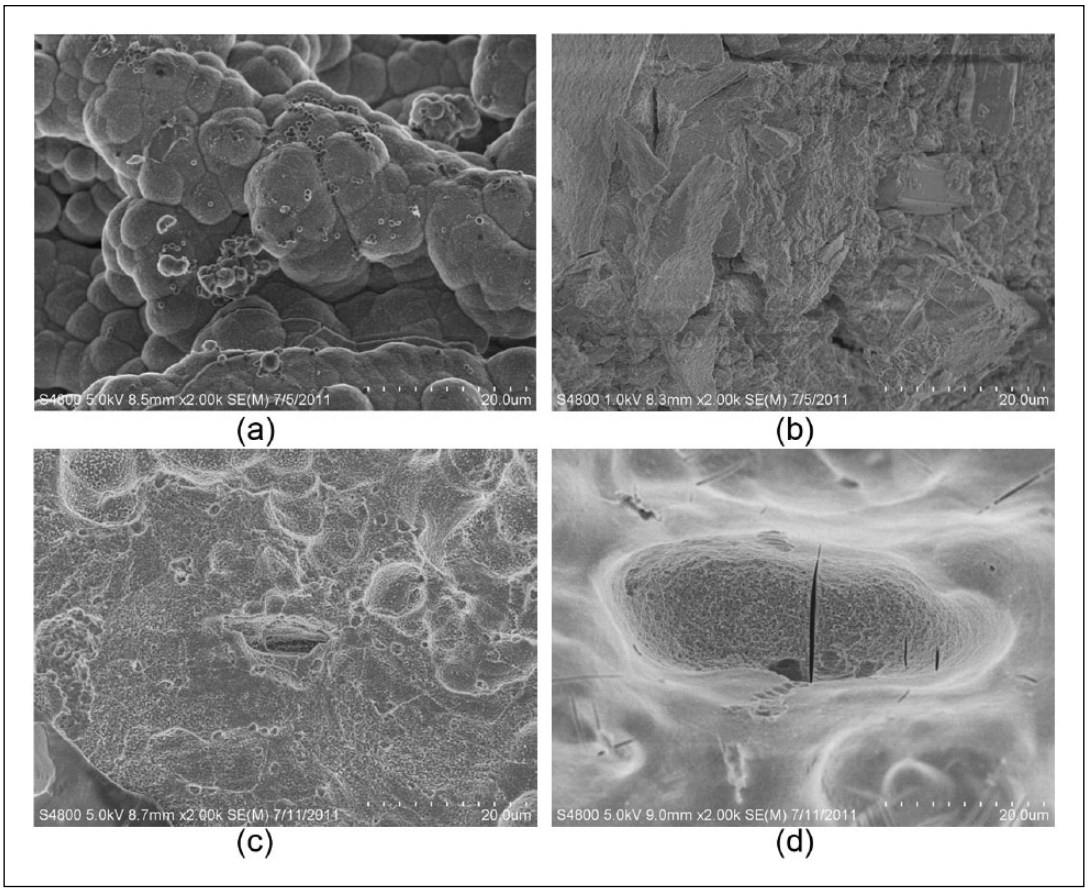

Figure 3. The in vitro corrosion morphology of the Ca–P-coated and uncoated AZ31 alloy. The surface of (a) the Ca–P-coated and (b) uncoated AZ31 alloy was rough with a layer of off-white corrosion products after a 30-day immersion in DMEM. The corrosion morphology of (c) the Ca–P-coated and (d) uncoated AZ31 alloy after removing the corrosion products, respectively.

Table 3. Elemental composition of the corrosion products on the surface of the Ca–P-coated and uncoated AZ31 alloy.

Ca–P coated AZ31 alloy			Uncoated AZ31 alloy		
Elements	Wt (%)	At (%)	Elements	Wt (%)	At (%)
O	46.83	59.55	O	49.35	24.33
C	8.19	13.88	C	15.29	56.20
Ca	26.23	13.32	Ca	11.03	5.26
P	12.91	8.48	P	4.79	2.96
Mg	4.41	3.68	Mg	7.28	5.72
Na	0.85	0.75	Al	9.45	1.25
Cl	0.58	0.34	Cl	2.81	1.52

Significantly more cells adhered to the surface of the Ca–P-coated AZ31 alloy samples than to the surface of the uncoated AZ31 alloy samples at 12 and 24 h (P <0.05).

Cell proliferation. The cell proliferation on the surface of the Ca–P-coated and uncoated AZ31 alloy samples are shown in Figure 7. In each group, the cell proliferation activity increased with culture time, indicating that a cell could attach and proliferate on the surface of the Ca–P-coated AZ31 alloy samples and on the surface of the uncoated AZ31 alloy samples.

In comparison with the uncoated AZ31 alloy, the number of cells on the surfaces of the Ca–P-coated AZ31 alloy showed a statistically significant increase on days 3 and 5 (P <0.05), indicating that the Ca–P-coated AZ31 alloy had

a significantly better surface bioactivity than the uncoated AZ31 alloy.

Blood cell aggregation. Aggregation of blood cells on the surface of the Ca–P-coated and uncoated AZ31 alloy samples is shown in Figure 8. As shown in Figure 8a, the reduction in RBC aggregation to the Ca–P-coated and uncoated AZ31 alloy was 20.46% and 19.90%, respectively. There was no significant RBC aggregation to the Ca–P-coated AZ31 alloy compared with uncoated AZ31 alloy (P >0.05). The reduction in WBC aggregation to the Ca–P-coated and uncoated AZ31 alloy was 26.24% and 31.21%, respectively (Figure 8b). The result demonstrated no significant aggregation of WBCs occurring on the Ca–P-coated AZ31 alloy compared with uncoated AZ31 alloy (P >0.05). As shown in Figure 8c, the reduction in platelet aggregation to the Ca–P-coated and uncoated AZ31 alloy was 23.22% and 19.03%, respectively. There was no significant platelet aggregation to the Ca–P-coated AZ31 alloy compared with uncoated AZ31 alloy (P >0.05). These results indicate that blood cells did not aggregate on the surface of the Ca–P-coated AZ31 alloy due to the excellent blood-compatible behavior.

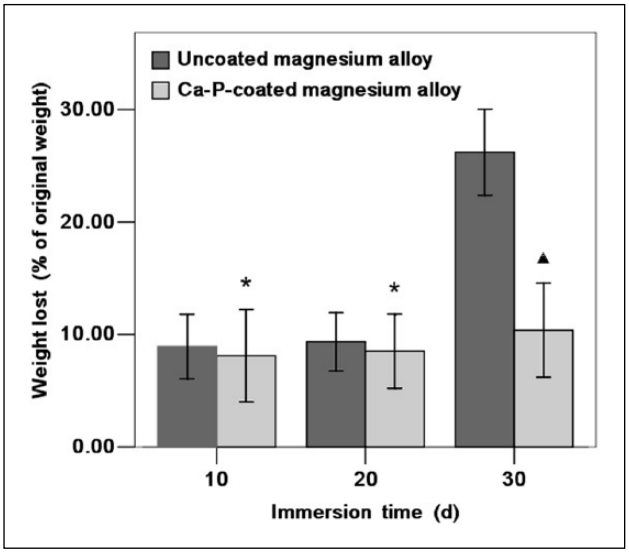

Figure 4. In vitro corrosion rates of the Ca–P coated and uncoated AZ31 alloy after 10, 20, and 30 days' immersion in DMEM cell culture medium. (▲P <0.05, *P >0.05).

Animal experiments

Radiographic evaluation. Figure 9 shows the radiographs of the New Zealand white rabbit tibias at 4, 8, and 12 weeks after surgery. No gas bubbles were observed after implantation in the Ca–P-coated AZ31 alloy group and all the implants were intact throughout the entire implantation period; however, there were generous gas bubbles around the implants in the uncoated AZ31 alloy group. In addition, based on X-ray radiographs, the corrosion of the Ca–P-coated AZ31 alloy plates was deepened as a function of implantation time. At week 4, the corrosion was not noticeable. The implant was blurred, but the size of the implant was not small at week 8. At week 12, the corrosion was noticeable, and the implant was blurred and the size of the implant was small. These results suggested that the Ca–P-coated AZ31 alloy might have been absorbed gradually in vivo; however, Ca–P coating significantly increased the corrosion resistance of the AZ31 alloy.

Blood analysis. Figure 10 shows the ALT, AST, CREA, BUN, and CK levels in the Ca–P-coated AZ31 alloy group, the uncoated AZ31 alloy group, and the sham-operated group after implantation. No significant differences were observed in the ALT, AST, CREA, BUN, and CK levels among the three groups prior to surgery (P >0.05). There were

Table 4. The optical density (OD) and relative cell growth rate (RGR) in different groups (n = 6).

Group	1 d		3 d		5 d	
	OD (mean ± SD)	RGR (%)	OD (mean ± SD)	RGR (%)	OD (mean ± SD)	RGR (%)
Negative	0.180 ± 0.027	100	0.323 ± 0.072	100	0.374 ± 0.062	100
25% extract	0.157 ± 0.042	87.2	0.354 ± 0.059*	109.6	0.415 ± 0.084†	111.0
50% extract	0.157 ± 0.016	87.2	0.351 ± 0.029*	108.7	0.380 ± 0.057†	101.6
75% extract	0.156 ± 0.032	86.7	0.334 ± 0.035*	103.4	0.369 ± 0.037†	98.7
100% extract	0.158 ± 0.026	87.8	0.331 ± 0.037*	102.5	0.387 ± 0.024†	103.5

*P <0.05 vs. 1 day.
†P <0.05 vs. 1 day.

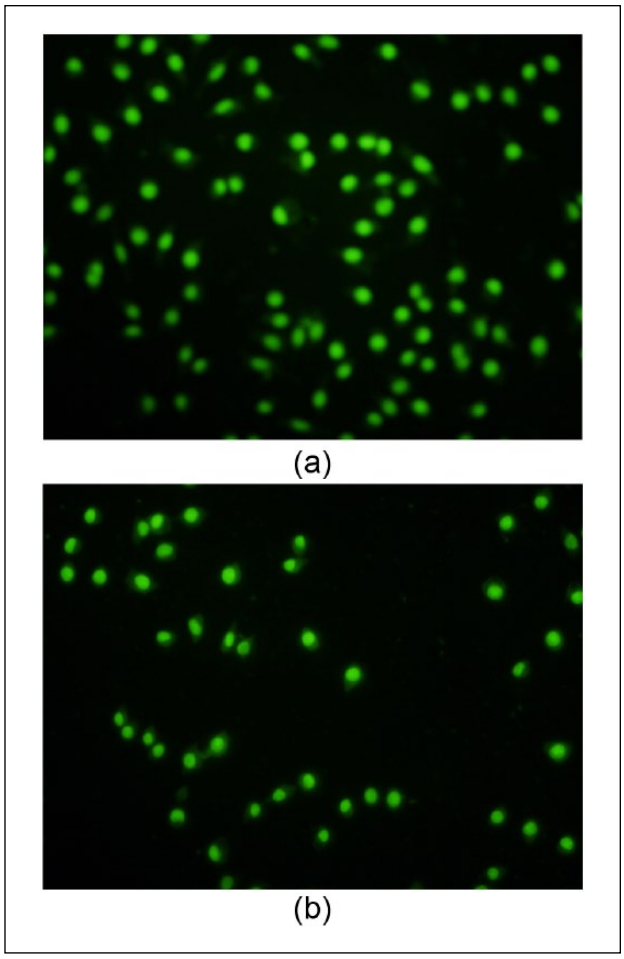

Figure 5. The adherent cells on the surface of (a) the Ca–P-coated and (b) uncoated AZ31 alloy samples after culture for 24 h (acridine orange staining). Magnification, ×400.

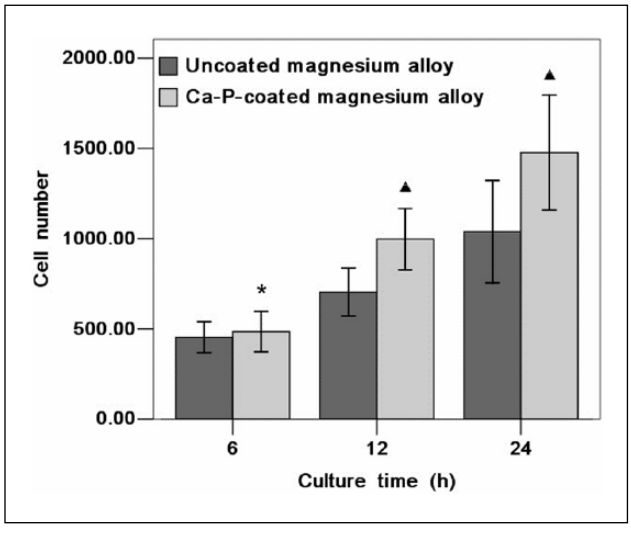

Figure 6. The number of adherent cells on the surface of the Ca–P-coated and uncoated AZ31 alloy samples after culture for 6, 12, and 24 h. (▲P <0.05, *P >0.05).

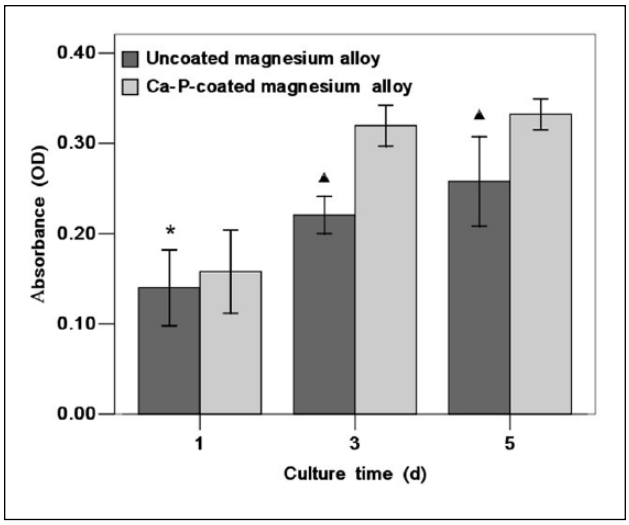

Figure 7. Cell proliferation on the surface of the Ca–P-coated and uncoated AZ31 alloy samples (▲P <0.05, *P >0.05).

no significant differences in the ALT, AST, CREA, and BUN levels among the three groups at the same time point following surgery (P >0.05), and no significant differences in the ALT, AST, CREA, and BUN levels at different time points in the same group following surgery (P >0.05). On day 1 after surgery, there was a rapid increase in the serum CK levels (P <0.05) in the three groups, which returned to the preoperative levels 28 days after the surgery; however, no significant differences were demonstrated among the three groups at the same time point after implantation (P >0.05).

Histopathologic examination. The New Zealand white rabbits were sacrificed at 4, 8, and 12 weeks after surgery and pathologic slices were obtained from the heart, liver, and kidneys (Figure 11). In the Ca–P-coated AZ31 alloy group, the hepatocytes were normal, with no remarkable inflammation or edema; the bile duct did not expand. The renal glomeruli and tubules had normal morphologies, without inflammatory cell infiltration. The structure of the myocardium was normal; no inflammation or necrosis was observed. In the uncoated AZ31 alloy group, hepatocytes did not exhibit significant swelling or necrosis, and the bile duct did not show expansion or bile siltation; no marked abnormalities existed in the central vein. The renal glomeruli had normal morphology and no edema or inflammation was detected. The morphology of the myocardium did not show substantial changes. In the sham-operated group,

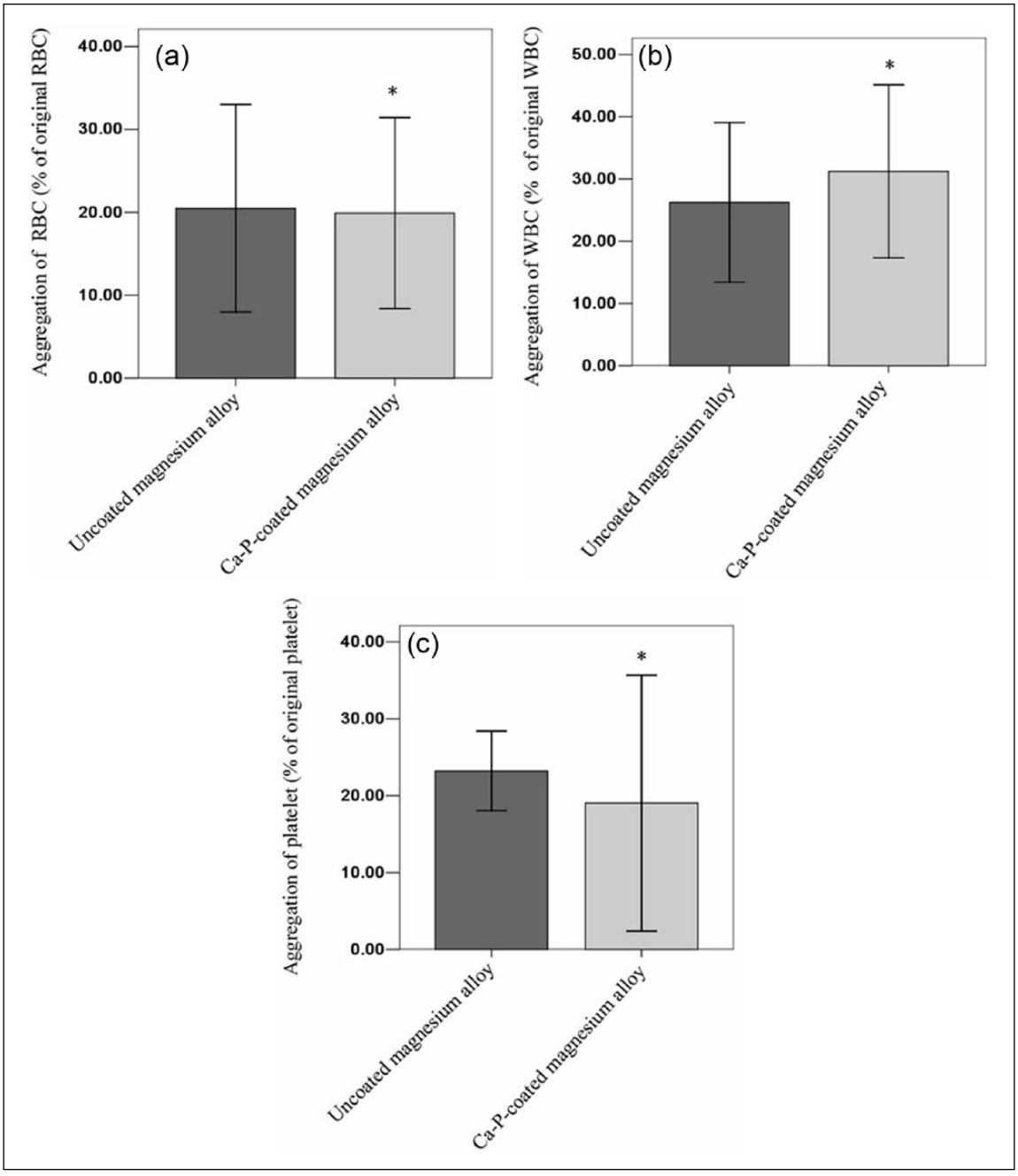

Figure 8. Comparison of aggregation of (a) RBCs, (b) WBCs, and (c) platelets on the surface of the Ca–P-coated and uncoated AZ31 alloy (*P >0.05).

regular tissue structure without signs of pathologic lesions was noted in all sections of the heart, liver, and kidneys.

Discussion

Recently, magnesium alloys were expected to be used in orthopedics as a revolutionary degradable metal biomaterial;[3,5,28] however, the high corrosion rate in physiologic solutions is a key factor limiting clinical application. It is well-known that alloying is a convenient and effective method to enhance the corrosion resistance of magnesium and its alloy.[29–31] A series of studies have reported that alloying has increased the corrosion resistance of magnesium alloys; however, the effect of alloying on controlling the corrosion rate might not be highly significant owing to the high electronegative potential of

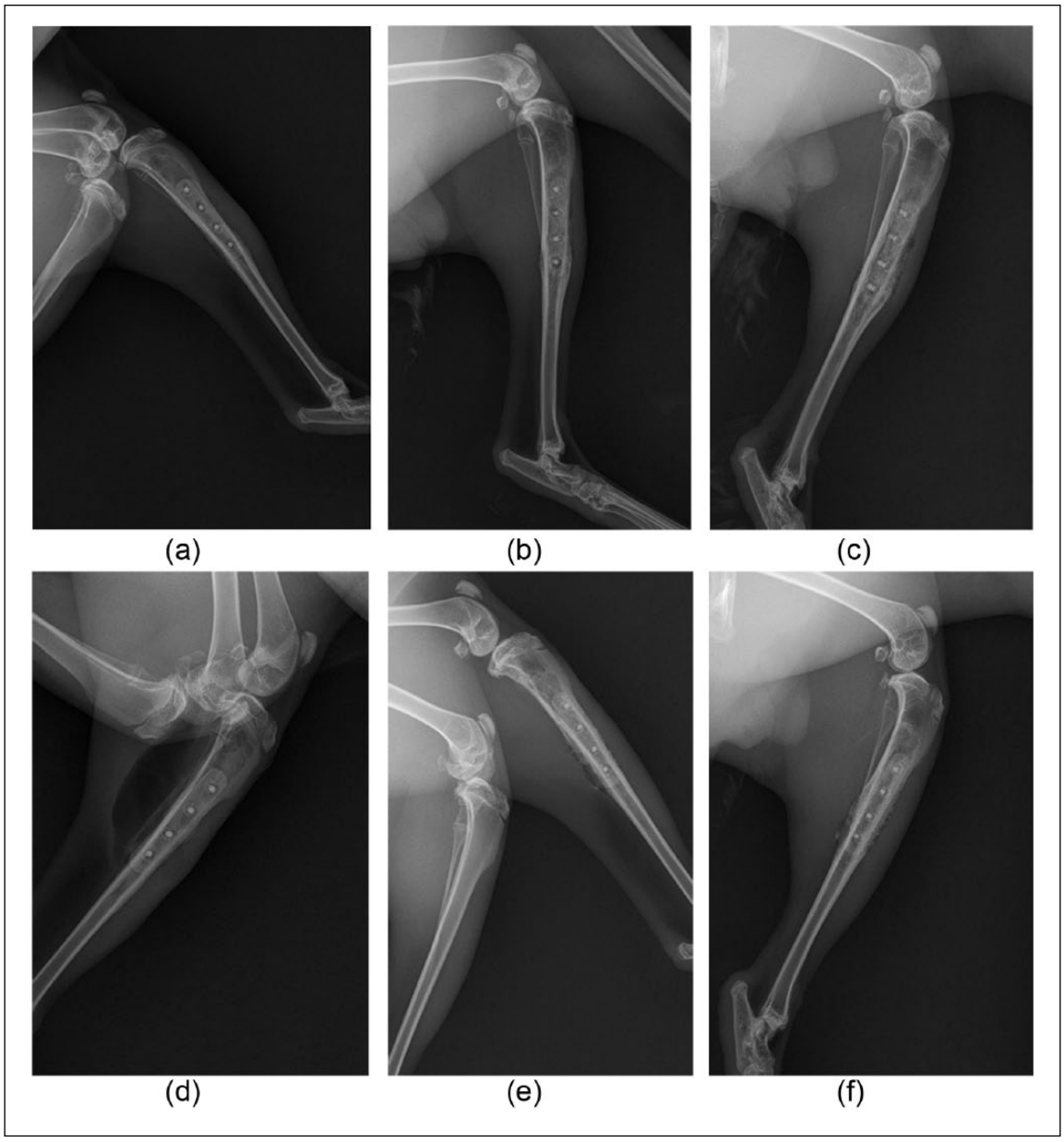

Figure 9. X-ray images of the implant region in the Ca–P-coated and uncoated AZ31 alloy groups at 4, 8, and 12 weeks postoperatively. (a–c) The Ca–P-coated AZ31 alloy plates implanted into the New Zealand white rabbit tibias at 4, 8, and 12 weeks after surgery. (d–f). The uncoated AZ31 alloy plates implanted into the New Zealand white rabbit tibias at 4, 8, and 12 weeks after surgery.

magnesium. Nevertheless, biocompatible coatings have been used to increase the corrosion resistance of magnesium alloys.[32–38] Not all coatings can be adapted for application on magnesium alloys, not only because of the high reactivity of magnesium and its relatively low melting temperature,[39] but also because of the toxicity which is unacceptable for biomedical application. In the current study, a Ca–P coating was fabricated on an AZ31 alloy by a chemical deposition process, and the surface structure and composition was investigated. To this end, we focused on the influence of the Ca–P coating on the corrosion behavior and surface biocompatibility of an AZ31 alloy.

Our primary concern regarding Ca–P coating on the surface of an AZ31 alloy is whether or not Ca–P coating can maintain the corrosion resistance during degradation. Before the Ca–P-coated AZ31 alloy was immersed in DMEM, SEM showed a Ca–P coating shaped like a flake on the

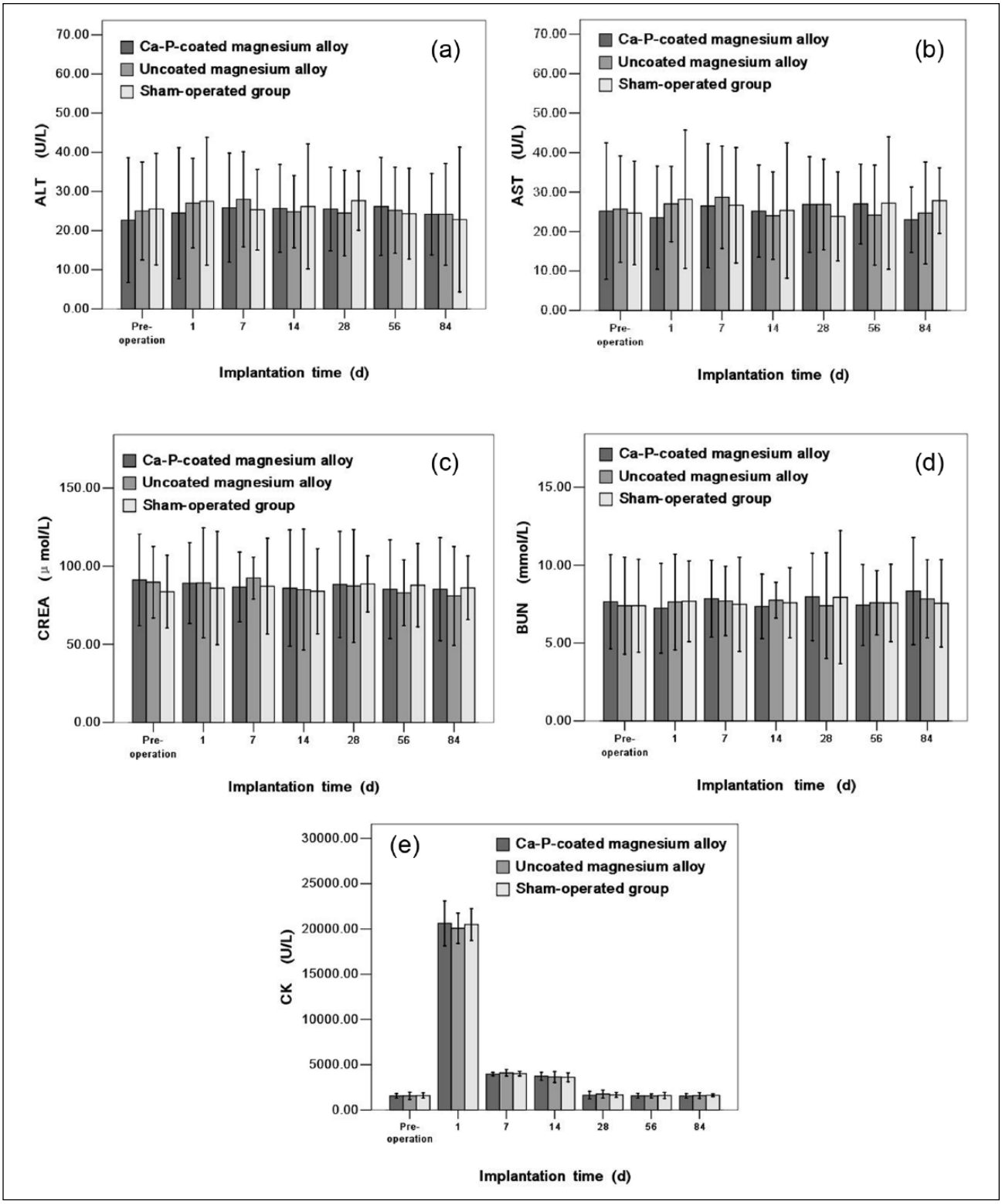

Figure 10. Results of serum (a) ALT, (b) AST, (c) CREA, (d) BUN, and (e) CK levels before and after implantation in each group.

surface of the AZ31 alloy, and the EDS results indicated that the particles were mainly composed of calcium, phosphate, oxygen, and carbon, suggesting that the Ca–P coating had the foundation of good surface biocompatibility. After 10, 20, or 30 days of static immersion in DMEM, the

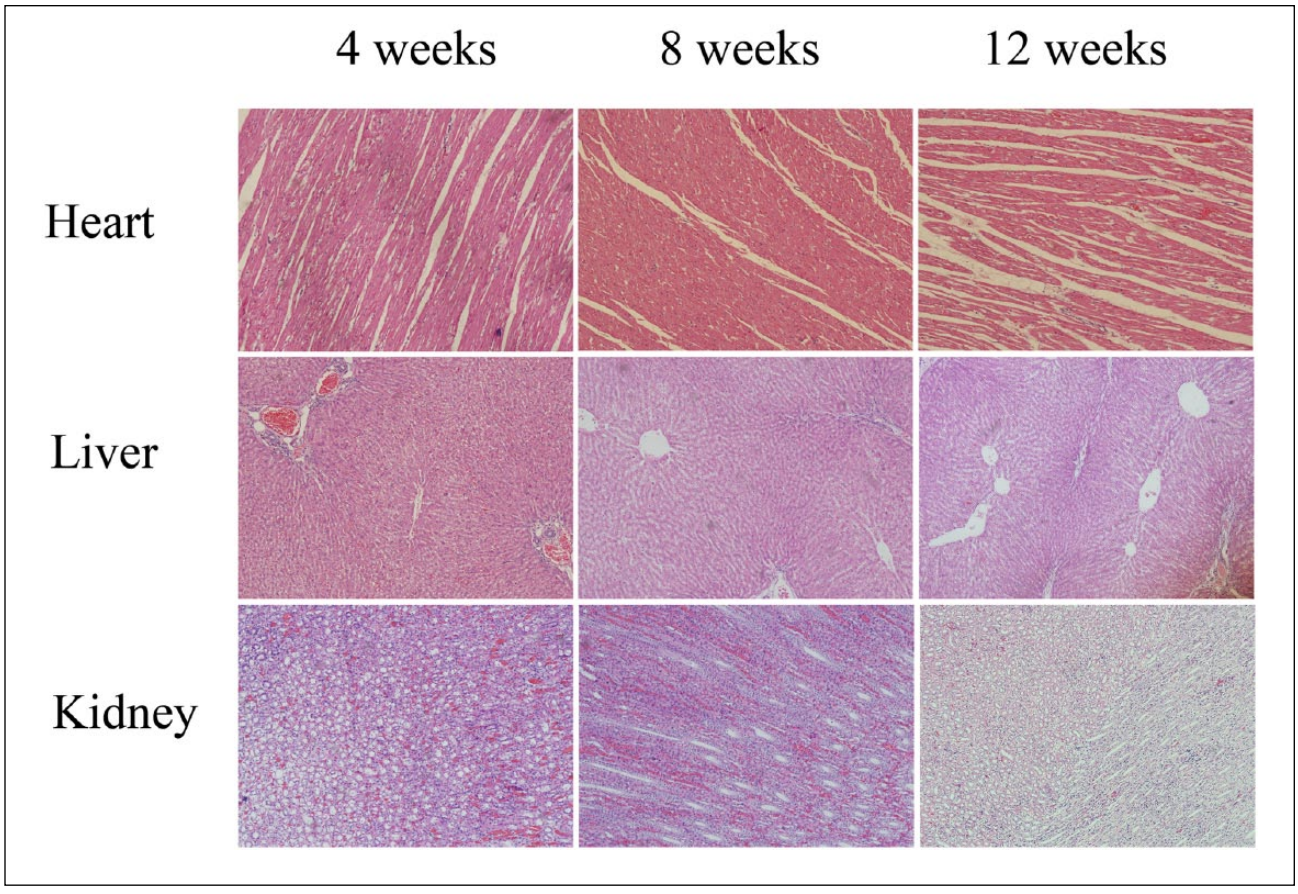

Figure 11. Pathologic photographs of the heart, liver, and kidneys after 4, 8, or 12 weeks post implantation (HE stained, ×100).

Ca–P-coated AZ31 alloy corroded much more slowly than the uncoated AZ31 alloy ($P < 0.05$), indicating that the Ca–P coating can increase corrosion resistance of the AZ31 alloy. Observations under SEM further identified the corrosion behavior of the Ca–P-coated AZ31 alloy according to corrosion morphology. The corrosion pits on the surface of the Ca–P-coated AZ31 alloy were smaller and more evenly distributed than those on the surface of the uncoated AZ31 alloy, indicating that the uncoated AZ31 alloy underwent severe pitting and general corrosion.

In agreement with the results of the immersion test, the in vivo animal study displayed similar results. Based on the radiographs, no gas bubbles were observed after implantation in the Ca–P-coated AZ31 alloy group; however, there were generous gas bubbles around the implants in the uncoated AZ31 alloy group. This phenomenon contributed to the high degradation rate of the uncoated AZ31 alloy, leading to the generation of generous hydrogen gas.

After surface modification, the corrosion resistance of the Ca–P-coated AZ31 alloy is mainly affected by the physical properties and the chemical properties of the surface coating. On the one hand, the corrosion resistance of the Ca–P-coated AZ31 alloy depends on the thickness of the surface coating. On the other hand, the integrity of the Ca–P coating also influences the corrosion rate. Therefore, the next step in our research will be to study the physical and chemical properties of the surface coating.

Another concern about Ca–P coating on the AZ31 alloy is whether or not Ca-P coating can improve the surface biocompatibility of Ca–P-coated AZ31 alloy. First, in vitro cytocompatibilities were assessed using cell experiments, including a cytotoxicity test, cell adhesion, and proliferation. The RGR of MC_3T_3-E_1 cells cultured in different extracts from the Ca–P-coated AZ31 alloy were all >75% at each time point, indicating that cytotoxicity was grade 0–1 at 1, 3, and 5 days. This suggested that the Ca–P-coated AZ31 alloy had no significant destructive effect on MC_3T_3-E_1 cells. Cell adhesion and

proliferation were significantly upgraded on the surface of the Ca–P-coated AZ31 alloy compared with the uncoated AZ31 alloy (P <0.05), indicating that the Ca–P coating significantly improved the surface bioactivity of AZ31 alloy as proposed. Indeed, it may be that the Ca–P-coated AZ31 alloy offers a biological environment for MC_3T_3-E_1 cells. On the one hand, the Ca–P coating on the surface of the AZ31 alloy, which does not include any toxic elements, is entirely biocompatible. On the other hand, the improved biological response of the Ca–P-coated AZ31 alloy to MC_3T_3-E_1 cells is believed to be closely related to a decreased corrosion rate. Normally, the cytotoxicity of magnesium alloys is due to the high corrosion rate, resulting in high cell osmolarity.[40,41] However, recent studies have shown that an appropriate magnesium ion concentration can lead to cell activation by regulation of protein synthesis and ancillary processes.[42,43] At the same time, calcium ions deposited on the surface of the Ca–P-coated AZ31 alloy may promote cell proliferation.[44–46] Taking these data together, the Ca–P-coated AZ31 alloy had no apparent cytotoxicity and could promote cell adhesion and proliferation without affecting normal function.

Subsequently, in vivo biocompatibilities were assessed using animal experiment. After the Ca–P-coated AZ31 alloy implants were implanted into New Zealand white rabbit tibias, the biocompatibilities were assessed by detection of ALT, AST, CREA, BUN, and CK levels in blood, and histopathologic analysis of the liver, kidneys, and heart at various time points. The serologic examination demonstrated that there were no significant differences in the ALT, AST, CREA, and BUN levels among the three groups at the same time point following surgery (P >0.05). There were no significant differences in the ALT, AST, CREA, and BUN levels at different time points in the same group following surgery (P >0.05). These results suggested that the implantation of the Ca–P-coated AZ31 alloy implants did not adversely affect the liver and renal function of New Zealand white rabbits. On the first day after surgery, there was a rapid increase in the serum CK levels (P <0.05) in the three groups, which returned to the preoperative levels 28 days after surgery; however, no significant differences were determined among the three groups at the same time point after implantation (P >0.05). Thus, the increased CK levels after surgery were induced by surgical factors, not by implantation of AZ31 alloy implants. Pathologic slices of liver, kidneys, and heart showed that the histologic structure did not change in the Ca–P-coated and the uncoated AZ31 alloy groups. This suggested that the Ca–P-coated the AZ31 alloy had excellent biocompatibility as degraded biomaterial implanted into the New Zealand white rabbit tibias. Although relatively rapid corrosion was found in the uncoated AZ31 alloy group, there were not serologic and pathologic changes, which suggested that there were no toxic effects on the blood, liver, kidneys, and heart. This was a good indication that the coated AZ31 alloy is safe for in vivo use, considering that once the coating on the AZ31 alloy is degraded completely, the uncoated AZ31 alloy will also degrade and not induce adverse effects on the blood, liver, kidneys, and heart.

The Ca–P-coated AZ31 alloy is absorbed gradually and has increased corrosion resistance and improved biocompatibility in vitro and in vivo. More importantly, the data indicated that after the Ca-P coating was degraded, the uncoated AZ31 alloy did not induce toxic levels. Of importance, there were some limitations to the current study. First, static immersion tests may not precisely simulate the actual physiologic conditions in the human body because the human body fluids circulate dynamically and ion concentrations vary in different parts of the human body.[47] In addition, although the Ca–P-coated AZ31 alloy had excellent biocompatibility in vitro and in vivo, further long-term in vivo studies, which continue until complete corrosion of the implant, are needed to validate and supplement our current data.

In this study, a Ca–P coating, mainly composed of calcium, phosphate, oxygen, and carbon, was successfully fabricated on the surface of an AZ31 alloy using a chemical deposition process. We showed that Ca–P coating can significantly increase the in vitro or in vivo corrosion resistance of an AZ31 alloy. In vitro studies showed that the Ca–P coating provided the AZ31 alloy with a significantly better cytocompatibility and hemocompatibility. In vivo results also confirmed that the Ca–P coating exhibited significantly improved biocompatibility within 12 weeks postoperatively. Collectively, the results generated in the present study indicate that Ca–P coating may successfully enhance corrosion resistance and improve surface bioactivity, suggesting that a Ca–P-coated AZ31 alloy could be a promising material for orthopedic applications.

Declaration of conflicting interests

The authors declared no potential conflicts of interest with respect to the research, authorship, and/or publication of this article.

Funding

This study was supported by the First Hospital Research Project of Lanzhou University (no. LDYYYN2013-01) and the National Natural Science Foundation of China (nos. 81271961 and 81572106).

References

1. Kirkland NT, Birbilis N and Staiger MP (2012) Assessing the corrosion of biodegradable magnesium implants: A critical review of current methodologies and their limitations. *Acta Biomaterialia* 8: 925–936.
2. Xin Y, Hu T and Chu PK (2011) *In vitro* studies of biomedical magnesium alloys in a simulated physiological environment: A review. *Acta Biomaterialia* 7: 1452–1459.
3. Witte F (2010) The history of biodegradable magnesium implants: A review. *Acta Biomaterialia* 6: 1680–1692.
4. Zhang S, Zhang X, Zhao C et al. (2010) Research on an Mg–Zn alloy as a degradable biomaterial. *Acta Biomaterialia* 6: 626–640.
5. Staiger MP, Pietak AM, Huadmai J et al. (2006) Magnesium and its alloys as orthopedic biomaterials: A review. *Biomaterials* 27: 1728–1734.
6. Li Z, Gu X, Lou S et al. (2008) The development of binary Mg-Ca alloys for use as biodegradable materials within bone. *Biomaterials* 29: 1329–1344.
7. Zberg B, Uggowitzer PJ and Löffler JF (2009) MgZnCa glasses without clinically observable hydrogen evolution for biodegradable implants. *Nature Materials* 8: 887–891.
8. Williams D (2006) New interests in magnesium. *Medical Device Technology* 17(3): 9–10.
9. Gu X, Zheng Y, Cheng Y et al. (2009) *In vitro* corrosion and biocompatibility of binary magnesium alloys. *Biomaterials* 30: 484–498.
10. Xu L, Yu G, Zhang E et al. (2007) In vivo corrosion behavior of Mg–Mn–Zn alloy for bone implant application. *Journal of Biomedical Materials Research. Part A* 83: 703–711.
11. Witte F, Kaese V, Haferkamp H et al. (2005) In vivo corrosion of four magnesium alloys and the associated bone response. *Biomaterials* 26: 3557–3563.
12. Walter R and Kannan MB (2011) *In vitro* degradation behaviour of WE54 magnesium alloy in simulated body fluid. *Materials Letters* 65: 748–750.
13. Hänzi AC, Gerber I, Schinhammer M et al. (2010) On the in vitro and in vivo degradation performance and biological response of new biodegradable Mg–Y–Zn alloys. *Acta Biomaterialia* 6: 1824–1833.
14. Salahshoor M and Guo YB (2011) Surface integrity of biodegradable magnesium-calcium orthopedic implant by burnishing. *Journal of the Mechanical Behavior of Biomedical Materials* 4: 1888–1904.
15. Park RS, Kim YK, Lee SJ et al. (2012) Corrosion behavior and cytotoxicity of Mg-35Zn-3Ca alloy for surface modified biodegradable implant material. *Journal of Biomedical Materials Research. Part B, Applied Biomaterials* 100: 911–923.
16. Wang Y, He Y, Zhu Z et al. (2012) *In vitro* degradation and biocompatibility of Mg-Nd-Zn-Zr alloy. *Chinese Science Bulleting* 57: 2163–2170.
17. Wang Y, Zhu Z, He Y et al. (2012) *In vivo* degradation behavior and biocompatibility of Mg-Nd-Zn-Zr alloy at early stage. *International Journal of Molecular Medicine* 29: 178–184.
18. Wang Y, Ouyang Y, Peng X et al. Effects of degradable Mg-Nd-Zn-Zr alloy on osteoblastic cell function. *International Journal of Immunopathology and Pharmacology* 25: 597–606.
19. Zhang S, Li J, Song Y et al. (2009) *In vitro* degradation, hemolysis and MC3T3-E1 cell adhesion of biodegradable Mg–Zn alloy. *Materials Science and Engineering C* 29: 1907–1912.
20. Xu L, Zhang E, Yin D et al. (2008) *In vitro* corrosion behaviour of Mg alloys in a phosphate buffered solution for bone implant application. *Journal of Materials Science. Materials in Medicine* 19: 1017–1025.
21. Wei J, Jia J, Wu F et al. (2010) Hierarchically microporous / macroporous scaffold of magnesium-calcium phosphate for bone tissue regeneration. *Biomaterials* 31: 1260–1269.
22. Yamamoto A, Watanabe A, Sugahara K et al. (2001) Improvement of corrosion resistance of magnesium alloys by vapor deposition. *Scripta Materialia* 44: 1039–1042.
23. Gray JE and Luan B (2002) Protective coatings on magnesium and its alloys–a critical review. *Journal of Alloys and Compounds* 336: 88–113.
24. American Society for testing and Materials (2004) ASTM-G31–72: Standard practice for laboratory immersion corrosion testing of metals. In: *Annual Book of ASTM Standards*. Philadelphia, PA: ASTM.
25. ISO 10993 (1999) *Biological Evaluation of Medical Devices – Part 5: Tests for Cytotoxicity: In Vitro Methods*. Switzerland.
26. ISO 10993 (2002) *Biological Evaluation of Medical Devices – Part 12: Sample Preparation and Reference Materials*. Switzerland.
27. Ito Y, Sisido M and Imanishi Y (1990) Adsorption of plasma proteins and adhesion of platelets onto novel polyetherurethaneureas-relationship between denaturation of adsorbed proteins and platelet adhesion. *Journal of Biomedical Materials Research* 24: 227–242.

28. Persaud-Sharma D and McGoron A (2012) Biodegradable magnesium alloys: A review of material development and applications. *Journal of Biomimetics, Biomaterials, and Tissue Engineering* 12: 25–39.
29. Kirkland NT, Birbilis N, Walker J et al. (2010) *In vitro* dissolution of magnesium-calcium binary alloys: Clarifying the unique role of calcium additions in bioresorbable magnesium implant alloys. *Journal of Biomedical Materials Research. Part B, Applied Biomaterials* 95: 91–100.
30. Kirkland NT, Lespagnol J, Birbilis N et al. (2010) A survey of bio-corrosion rates of magnesium alloys. *Corrosion Science* 52: 287–291.
31. Witte F, Fischer J, Nellesen J et al. (2006) *In vitro* and *in vivo* corrosion measurements of magnesium alloys. *Biomaterials* 27: 1013–1018.
32. Yang J, Cui F and Lee IS (2011) Surface modifications of magnesium alloys for biomedical applications. *Annals of Biomedical Engineering* 39: 1857–1871.
33. Li GY, Lian JS, Niu LY et al. (2006) Growth of zinc phosphate coatings on AZ91D magnesium alloy. *Surface and Coatings Technology* 201: 1814–1820.
34. Zhao M, Wu S, An P et al. (2006) Microstructure and corrosion resistance of a chromium-free multi-elements complex coating on AZ91D magnesium alloy. *Materials Chemistry and Physics* 99: 54–60.
35. Wang YQ, Wu K and Zheng MY (2006) Effects of reinforcement phases in magnesium matrix composites on microarc discharge behavior and characteristics of microarc oxidation coatings. *Surface and Coatings Technology* 201: 353–360.
36. Thorey F, Menzel H, Lorenz C et al. (2011) Osseointegration by bone morphogenetic protein-2 and transforming growth factor beta 2 coated titanium implants in femora of New Zealand white rabbits. *Indian Journal of Orthopaedics* 45: 57–62.
37. Aykut S, Ozturk A, Ozkan Y et al. (2010) Evaluation and comparison of the antimicrobial efficacy of teicoplanin- and clindamycin-coated titanium implants: An experimental study. *Journal of Bone and Joint Surgery. British volume* 92: 159–163.
38. Kazemzadeh-Narbat M, Kindrachuk J, Duan K et al. (2010) Antimicrobial peptides on calcium phosphate-coated titanium for the prevention of implant-associated infections. *Biomaterials* 31: 9519–9526.
39. Wen C, Guan S, Peng L et al. (2009) Characterization and degradation behavior of AZ31 alloy surface modified by bone-like hydroxyapatite for implant applications. *Applied Surface Science* 255: 6433–6438.
40. Witte F, Hort N, Vogt C et al. (2008) Degradable biomaterials based on magnesium corrosion. *Current Opinion in Solid State and Materials Science* 12: 63–72.
41. Song GL (2007) Control of biodegradation of biocompatible magnesium alloys. *Corrosion Science* 49: 1696–1701.
42. Rude RK, Gruber HE, Wei LY et al. (2003) Magnesium deficiency: Effect on bone and mineral metabolism in the mouse. *Calcified Tissue International* 72: 32–41.
43. Harry R (2005) Magnesium: The missing element in molecular views of cell proliferation control. *Bioassays* 27: 311–320.
44. Yamaguchi M, Oishi H and Suketa Y (1987) Stimulatory effect of zinc on bone formation in tissue culture. *Biochemical Pharmacology* 36: 4007–4012.
45. Villa I, Dal Fiume C, Maestroni A et al. (2003) Human osteoblast-like cell proliferation induced by calcitonin-related peptides involves PKC activity. *American Journal of Physiology. Endocrinology and Metabolism* 284: E627–633.
46. Cheng K, Weng W, Wang H et al. (2005) *In vitro* behavior of osteoblast-like cells on fluoridated hydroxyapatite coatings. *Biomaterials* 26: 6288–6295.
47. Lévesque J, Hermawan H, Dubé D et al. (2008) Design of a pseudo-physiological test bench specific to the development of biodegradable metallic biomaterials. *Acta Biomaterialia* 4: 284–295.